Journal Pre-proof

Phytic Acid Functionalized Antifouling Conducting Polymer Hydrogel for Electrochemical Detection of MicroRNA

Lili Yang, Hao Wang, Haitao Lü, Ni Hui

PII: S0003-2670(20)30560-2

DOI: https://doi.org/10.1016/j.aca.2020.05.025

Reference: ACA 237666

To appear in: *Analytica Chimica Acta*

Received Date: 2 January 2020

Revised Date: 5 May 2020

Accepted Date: 10 May 2020

Please cite this article as: L. Yang, H. Wang, H. Lü, N. Hui, Phytic Acid Functionalized Antifouling Conducting Polymer Hydrogel for Electrochemical Detection of MicroRNA, *Analytica Chimica Acta*, https://doi.org/10.1016/j.aca.2020.05.025.

Author contributions

Lili Yang: Conceptualization, Methodology, Software, Investigation, Writing Original Draft.

Hao Wang: Validation, Formal analysis, Visualization, Software.

Haitao Lü: Validation, Formal analysis, Visualization.

Ni Hui: Resources, Writing - Review & Editing, Supervision, Data Curation.

Graphical abstracts

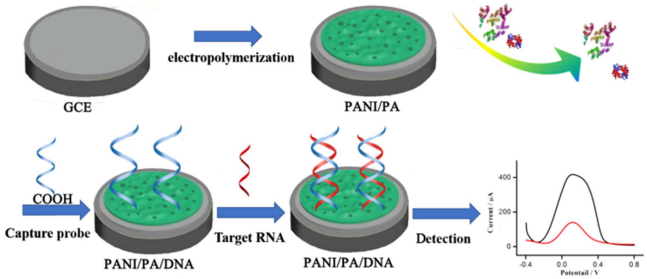

An electrodeposition method was used to prepare polyaniline (PANI) based conducting polymer hydrogel through the assembly of PANI and phytic acid (PA) by dynamic boronate bond. The biosensor based on PANI/PA hydrogel has shown excellent sensing performances with wide linear range (1.0 fM-1.0 pM) and low sensing limit (0.34 fM).

Phytic Acid Functionalized Antifouling Conducting Polymer Hydrogel for Electrochemical Detection of MicroRNA

Lili Yang, Hao Wang, Haitao Lü, and Ni Hui*

College of Chemistry and Pharmaceutical Sciences, Qingdao Agricultural University, Qingdao 266109, China

* Corresponding author. Tel: + 86 532 86080374; Fax: + 86 532 86080452; E-mail: huini1029@163.com

Absract： A rapid, sensitive and low-fouling sensor for application to detect clinical biomarkers directly in biological media is highly desirable. Herein, we report a versatile strategy to prepare polyaniline (PANI) based conducting polymer hydrogel through the assembly of PANI and phytic acid (PA) by dynamic boronate bond. PANI/PA, a conductive hydrogel with high specific area and multiple pore structures have demonstrated excellent antifouling ability and electrochemical property. The electrochemical biosensors for microRNA can be developed by the immobilization of DNA probes onto PANI/PA interface (microRNA24 is used as a model case), and redox currents of PANI were utilized as the sensing signals to assay DNA/RNA hybridization reaction. Owing to the typical characteristics of PANI/PA hydrogel, the biosensor has shown excellent sensing performances with wide linear range (1.0 fM-1.0 pM), low sensing limit (0.34 fM), and efficient ability to detect microRNA mismatches. Given the facile processability, excellent stability and good antifouling property of the PANI/PA hydrogel, the proposed hydrogel-based biosensor may find broad applications in clinical diagnostics and biomedical devices.

Keywords: Conducting polymer hydrogel; Polyaniline; Phytic acid; Antifouling; Nonspecific adsorption; Biosensor

1. Introduction

Disease diagnostic methods are required to be rapid, sensitive, specific, and economical [1, 2]. MicroRNAs (miRNAs), approximately 19-23 nucleotides, are a large group of small RNAs related to tumour transformation [3], stem cell regeneration [4] and viral spread [5]. MiRNAs are also emerging biomarkers that can show the occurrence of disease and predict the prognosis of the disease. For the assay of miRNAs, their properties, such as short sequence, high similarity in size and low concentration, cause great difficulty using conventional strategies including Northern blotting [6, 7] and polymerase chain reaction (PCR) [8]. Lots of new technologies, such as colorimetric assay [9, 10], fluorescence technology [11, 12], electrochemical assay [13-15], have been established to improve the sensitivity and applicability of the measurement. Among these ways, electrochemical sensors have received more and more attentions due to their merits (low test cost, simple instrument operation, fast test data and high sensitivity) [16].

Due to the serious nonspecific adsorption and biological penetration of complex biological media, the practical clinical application of biosensors still remains enormous challenges [2]. Therefore, depressing nonspecific protein adsorption on the sensor interfaces is very important for the application of biosensors in complex samples, and many attempts have been made to solve the problem. It is well known that surface hydrophilization is crucial to the improvement of interfacial antifouling ability [17]. The self-assembled antifouling monolayer [18] was utilized to modify the surface of the polymer layer [19] and the polymer brush [20] to inhibit the adhesion of

nonspecific proteins. For example, a label-free electrochemical DNA sensor based on self-assembled antifouling peptide layer was constructed for the direct assay of breast cancer marker BRCA1 in human serum samples [21]. Polyethylene glycol (PEG), a hydrophilic polymer grafted onto the surface of polyaniline (PANI), has been used to determine DNA in human serum [22]. However these antifouling interfaces have many preparation steps and the process is relatively complicated. Therefore, it is of great significance to develop antifouling materials that can deposit antifouling coatings directly through simple, scalable and economical synthesis methods.

Conductive polymer hydrogels, owing to their excellent biocompatibility, high electrical conductivity, three-dimensional nanostructures, and large specific surface area, have been employed as bases for the preparation of electrochemical sensors [23]. Hydrogels are polymeric networks that have a high level of hydration and three-dimensional (3D) microstructures bearing similarities to natural tissues [24]. Hydrogels based on conducting polymers (e.g., polythiophene, polyaniline, and polypyrrole) represent a novel polymeric material platform that synergizes the advantages of both organic conductors and hydrogels [25-26]. Among numerous conducting polymer hydrogels, PANI-based hydrogels have received extensive concerns because they own lots of promising properties including excellent mechanical properties, label free, high electronic conductivity, reversibility in redox, and good biocompatibility [27-30]. In addition, the amino group of PANI ($-NH_2$) can be easily modified with biomacromolecules, making it very desirable for biosensor construction. Moreover, the antifouling material is inspired by hydrophilicity to

construct the interface of the biosensor. Phytic acid (PA) is an ecologically friendly, renewable, abundant biomass, which is easily gained from grains [31-33]. The six phosphate groups supply all kinds of feasible crosslinking sites that may “suture” many conducting polymers sheets, forming the three-dimensional assembly body [34]. In previous reports, PA was used to construct a super-hydrophilic interface. For instance, Zhao's group reported the use of PA to construct a super-hydrophilic coating in a one-step assembly process [35]. Herein, a conductive polymer hydrogel with good antifouling property was synthesized by one-step electrochemical method with 3-aminobenzene boric acid (ABA) as crosslinking agent, PA doped PANI.

In this work, we aim to construct a novel PANI/PA conducting polymer hydrogel by one-step electrochemical copolymerization way. Boronic acid groups were covalently inserted into PANI chains through aggregating of 3-aminophenylboronic acid (ABA) and aniline [30, 36]. Boronic acid as the functional group has been chosen to crosslink PA and PANI at molecular level to form PANI/PA hydrogel [30]. The gelation mechanism of PANI/PA hydrogel is illustrated in Figure 1. The resulting PANI/PA conducting polymer hydrogel, combining strong hydrophilicity and biocompatibility of PA with the good electrochemical property of PANI, supply a good base for the development of antifouling electrochemical sensors. MiRNA24 was used to be a model case, which plays important roles in cancer cell proliferation and differentiation. As shown in Scheme 1, the DNA probes were attached onto the surface of the synthesized PANI/PA hydrogel by covalent bond modification to

construct an electrochemical biosensor with both antifouling property and good selectivity for miRNA24.

Scheme 1.

2. Experimental

2.1. Reagents and apparatus

Aniline, PA, ABA, sodium phosphate monobasic dihydrate (NaH_2PO_4), sodium phosphate dibasic dodecahydrate ($Na_2HPO_4 \cdot 12H_2O$), N-hydroxysuccinimde (NHS), 1-ethyl-3-(3-dimethylaminopropyl) carbodiimide (EDC), were bought from Aladdin regent (Shanghai, China). Hemoglobin from bovine blood (BHb), bovine serum albumin (BSA), albumin human serum (HSA), lysozyme (Lys) and diethyl pyrocarbonate (DEPC)-treated water were purchased from Beijing solibao technology Co. Ltd (Beijing, China). The synthetic 5′-carboxyl group terminated DNA capture probe, miRNA24 (T), miRNA21 (M1), three-based mismatch miRNA24 (M2) and single-based mismatch miRNA24 (M3) were obtained from Shanghai Shenggong co. LTD (Shanghai, China). And the base sequences of the DNA and miRNAs are shown in the supporting information.

2.2. Apparatus

All electrochemical measurements were carried out with a CHI660E Electrochemical Workstation (Shanghai CH Instrument Co., China) at room temperature with conventional three-electrode system consisted of glassy carbon electrode (GCE, 3.0 mm in diameter) as the working electrode, a platinum wire as a counter electrode, and a saturated calomel electrode (SCE) as the reference electrode.

Scanning electron microscope (SEM) with the model of JEOL JSM-7500F (Hitachi High Technology Co., Ltd., Japan) was used to characterize nanostructures and morphologies of prepared PANI and PANI/PA nanomaterials. X-Ray photoelectron spectroscopy (XPS) analysis was performed using a Thermo-VG Scientific ESCALAB 250 spectrometer with a Al monochromatic source operated at a voltage of 15 kV. Fourier transform infrared spectroscopy (FTIR) was carried out using a Nicolet iS10 spectrometer made by Syme fisher company (United States). The fluorescence was monitored using TCS SP5 confocal laser microscope (Leica, Germany). Static water contact angle measurements (CA) were carried out using a DSA25 goniometer (KRÜSS GmbH, Germany).

2.3. Synthesis of PANI/PA hydrogels

Before use, GCE was polished according the method previously reported [22]. PANI/PA hydrogels were electrochemical prepared through a galvanostatic way onto the surface of GCEs. The electrochemical polymerization was finished at a constant current density (0.01 mA cm^{-2}) for 60 minutes at room temperature, and the deposition solution was 1.0 M HCl solution containing 1 M aniline, 0.05 M ABA and 0.2 M PA. Meanwhile, the pure PANI hydrogel was prepared by the same electrochemical deposition method. And the deposition solution was 1.0 M HCl solution containing 1 M aniline, 0.05 M. The PANI/PA containing $-NH_2$ groups can be utilized for the following covalent attachment of DNA probe, and its electrochemical redox signals can be utilized as the detection signals of the prepared

biosensor [37]. Cyclic voltammetry (CV) technique was used to assess the stability of PANI/PA nanomaterial interface.

2.4. Characterization of PANI/PA antifouling property

In order to monitor the antifouling property of PANI/PA interface, single protein solutions and real media were examined. Differential pulse voltammetry (DPV) technique was employed to monitor the nonspecific adsorption of electrode surfaces before and after soaking in single protein solution or complex media (30 min). At the same time, we use fluorescence imaging technology to display the antifouling performance of the interface more intuitively. Both bare electrode and pure PANI modified GCE were utilized as controls. All interfaces were soaked in fluorescein isothiocyanate labelled bovine serum albumin solution (FITC-BSA, 0.1 mg mL^{-1}) for 30 minutes and gently washed with PBS and pure water thoroughly three times respectively. Finally, the visions of these interfaces were obtained by a confocal fluorescence microscope.

2.5. Immobilization of capture probe

PANI/PA modified electrodes (GCE/PANI/PA) were soaked in 1.0 μM carboxyl-functionalized DNA probe solution (configured with 0.2 M PBS, pH 7.4) containing 0.4 M EDC, 0.1 M NHS for 1 h at room temperature. In this process, DNA probes were covalently bonded with amino groups of PANI/PA. GCE/PANI/PA/DNA was successfully achieved. The synthetic PANI/PA conducting polymer hydrogel has

many amine groups on the surface. The DNA probes have been modified with carboxyl groups. The immobilization of DNA probes on the PANI/PA hydrogel were completed by covalent binding between carboxyl group of DNA probes and the amine groups of PANI/PA conducting polymer hydrogel using EDC and NHS as coupling reagents. The chemical reaction mechanism has been shown in Scheme S1.

2.6. Sensing with the biosensor

The DPV technique was carried out to monitor the specific bio-recognition activities on GCE surfaces, recording in PBS (pH 5.7) in the range of -0.4 to 0.8 V, with the pulse width of 0.05 s and the amplitude of 0.05 V. The constructed biosensor was soaked in different concentrations of miRNA24 solution for 45 minutes at ambient room temperature. To test the specificity of the assay, M1, M2 and M3 were used as controls.

3. Results and discussion

3.1. Characterization of PANI/PA hydrogels

As shown in Figure 1A, when a constant oxidation current passes through a colourless solution of PA, aniline, and ABA, a dark hydrogel formed quickly onto the GCE surface (Figure 1B left). Boronic acid groups were covalently installed on a PANI chain by copolymerization of 3-aminophenylboronicacid (ABA) and aniline (AN) (Figure 1A) [30]. The intermolecular interaction between boronic acid groups on PANI and hydroxyl groups on PA serves as the crosslink between PANI and PA,

resulting with a quick gelation (Figure 1B). Notably, without ABA, aniline and PA cannot form hydrogels under the same electrochemical oxidation conditions. ABA is crucial to the formation of PANI/PA hydrogels. The microstructure and surface morphology of PANI/PA hydrogels were characterized by SEM. As shown in Figure 1B, PANI/PA hydrogels exhibit a hierarchical porous structure consisted of clustered nanosphere with uniform diameters of 0.5-0.8 μm. Moreover, it can be clearly observed from Figure 1 that the surface of nanospheres presents a relatively smooth and flat feature, which is beneficial to enhance the antifouling properties of hydrogels [38]. As the substrate nanomaterial for biosensor, the newly obtained hydrogels with excellent antifouling performance, porous structure, high specific surface area, and label free are favourable to use as an ultrasensitive biosensor.

The successful synthesis of PANI/PA was proved using FTIR. Figure 2A shows the FTIR spectra of (a) PANI and (b) PANI/PA conductive polymer hydrogels. PANI (curve a) and PANI/PA (curve b) also showed absorption bands at 1450, 1594 and 1645 cm^{-1} (C=C stretching deformation of quinoid), 1278 and 1299 cm^{-1} (C-N stretching of the secondary aromatic amine), 3425 cm^{-1} (N-H stretching modes) and 849 cm^{-1} (C-H out of plane bending vibration) [39]. As expected, for the FTIR spectrum of PANI/PA (curve b), new bands appear at 1454, 1563 and 2928 cm^{-1}, which are ascribed to hydroxyl bands [40]. In summary, these results confirmed that PANI/PA conducting polymer hydrogel, with a large number of hydroxyl groups on the surface, has been successfully synthesized. The FTIR spectra suggested that PANI/PA conductive polymer hydrogel was successfully synthesized. Moreover,

wetting property and hydrophilicity of newly designed hydrogels were measured by static water contact angle. As shown in Figure 2C and Table S1, static water contact angle of PANI/PA hydrogels (17.9°) is significantly lower than those of bare electrode (70.9°) and PANI (55.5°). It is worth noting that when PA was doped into PANI, the hydrophilic property of PANI/PA is significantly increased comparing with pure PANI. The obvious hydrophilicity enhancement of PANI/PA can successfully improve the antifouling property of the nanomaterial [38, 41].

The stability analysis of PANI/PA hydrogel was detected by continuous CV tests in PBS (0.2 M, pH 5.7) with the potential range from -1 to 1 V. As shown in Figure 2B, a sharp oxidation peak at about 0.3 V and a reduction peak at about 0.08 V were observed for the PANI/PA conductive polymer hydrogel modified GCE due to the oxidation and reduction of PANI [37]. Clearly, the transducing signal is obviously unchanged after 50 cycles. The results showed that PANI/PA, a synthesized conductive polymer hydrogel, had good stability as the substrate of biosensor. In summary, we have synthesized a porous, hydrophilic and stable conductive polymer hydrogel.

Fig. 1

Fig. 2

XPS analysis was employed to evaluate the successful copolymerization of PANI/PA as well as the immobilization of DNA capture probe. As illustrated in Figure 3A, strong signals (at 284, 399, and 531 eV) of PANI XPS pattern are assigned to C (1s), N (1s), and O (1s), respectively, which is the typical characteristic of PANI

[42]. As shown in Figure 3B, after incorporation of PA and ABA, the O 1s peak greatly enhanced, together with the emergence of P 2p peak (from PA) and B 1s peak (from ABA), confirming the successful copolymerization of PANI with both ABA and PA. As shown in Figure 3C and Table S2, the quantified XPS results of PANI, PANI/PA and PANI/PA/DNA display the atomic composition of P 2p and N 1s. The increase of both P 2p and N 1s of PANI/PA/DNA confirmed the successful modification of DNA probe onto the PANI/PA hydrogel (Table S2).

Fig. 3

3.2. Evaluation of nonspecific protein adsorption of PANI and PANI/PA

In order to inspect the antifouling property of different modified surfaces, we fabricated PANI and PANI/PA hydrogel to compare the antifouling property in various single protein solution (BHb, BSA, HSA, Lys). In a typical experiment, the modified electrodes were immersed in PBS (0.2M, pH 5.7) to establish stable DPV base responses, and then their DPV responses were recorded in the same PBS again after incubation in aqueous solutions with 10^{-6} g $mL^{-1}$of different proteins for 30 min, respectively. As shown in Figure 4, after immersion in different protein solution (30min), the changes of DPV response of GCE/PANI/PA are much smaller than those of pure GCE/PANI. This is because a large amount of protein can adsorb onto the pure PANI surface, and these protein biomacromolecules hinder the electron transfer of the surface [43]. Compared with pure PANI, the conductive polymer hydrogel PANI/PA can effectively prevent the adverse effects caused by such nonspecific

adsorption. Moreover, the antifouling ability of pure PANI and PANI/PA hydrogel modified surfaces were further investigated using FITC-BSA (Figure 5), where almost no visible FITC-BSA is obvious at the PANI/PA interfaces. All results demonstrate excellent antifouling capability of the PANI/PA hydrogel interface towards single protein.

Fig. 4

Fig. 5

Besides single protein solutions, two complex biological media including bovine serum and milk samples were used to further evaluate the antifouling performance of the synthesized hydrogel. As shown in Figure S1, after serum or milk immersions (30 min), the decreases of DPV response of PANI/PA surfaces were significantly smaller than those of pure PANI surfaces, proving antifouling capability of PANI/PA hydrogel.

3.3. Characterization of the PANI/PA hydrogel-based biosensor

In order to efficiently characterize stepwise of the GCE/PANI/PA/DNA (Figure 6), the corresponding CV and DPV were performed in the absence of solution phase oxidation-reduction probes (PBS 5.7). From Figure 6A, CV curves show a well-defined redox peak, which could be contribute to the redox of PANI [37]. As expected, after the immobilization of DNA capture probes on the surface of hydrogel matrix, an obvious decrease of peak currents is observed (curve b), which is due to the fact that most biological macromolecules (including DNA) are low electron transfer

and can cause hindrance to the charge transfer [44]. The peak current of the biosensor decrease after the specific binding of target (miRNA24) again, because the electrostatic repulsion of double stranded DNA/RNA severely restrict the electron transfer of the biosensor. Therefore, based on the specific probes-target reaction, an ultrasensitive miRNA24 biosensor has been successfully constructed. The biosensor construction process was also monitored using DPV (Figure 6B). Undoubtedly, after DNA probes and miRNA targets were immobilized onto the PANI/PA surface, a successive decrease of the current (a-c) was detected. All DPV results are consistent with CV results, which prove the successful construction of miRNA biosensor with ultrasensitive electrochemical response changes.

The CV technology was measured to investigate the charge transport characteristics of GCE/PANI/PA at different scan rates. It is shown in Figure 6 (C and D) that the slight peak potential changes with the increase in scan rate. The anodic and cathodic peak currents of the modified electrode increases with the increase of scan rates. The linear regression equation between the anodic peak current and scan rate is $I / \mu A = 3775.59\ v + 1066.20$ (R^2=0.9957) (R^2 = 0.998) with the range from 0.1 to 2.5 V s^{-1}. The linear regression equation between the cathodic peak current and scan rate is $I / \mu A = -2031.35\ v - 950.78$ (R^2=0.9978) with the range from 0.1 to 2.5 V s^{-1}. The results demonstrated that the redox process of the GCE/PANI/PA surface is adsorption-controlled process.

Fig. 6

3.4. Optimization of conditions for the miRNA detection

GCE/PANI/PA/DNA has been optimized to improve miRNA24 detection performance. The electrodeposition time of PANI/PA hydrogel, the immobilization time of DNA probes onto GCE/PANI/PA and the hybridization time between miRNA24 and DNA were taken as important parameters of the analysis method, which were investigated in detail. The experimental results and discussion have been shown in the supporting information (Figure S2). The electrodeposition time of PANI/PA hydrogel has been selected as 60 min. The immobilization time of DNA probes was optimized for 60 min. The hybridization time between miRNA24 and DNA has been selected as 45 min.

The DPV parameters optimization has been shown in Figure S3. The experimental results show that the optimal setting parameters are as follows: increase E is 0.004 V; amplitude of 0.05 V; pulse width of 0.05 s; pulse period of 0.5 s. At the conditions, the peak current of DPV is the largest, which is beneficial to improve the sensitivity of the method.

3.5. Analytical performance of the miRNA24 biosensor

The biosensing achievements of the proposed GCE/PANI/PA/DNA for label free determination of target miRNA24 related sequence was assessed in PBS (0.2 M, pH 5.7) by DPV tests. The incubation time of the biosensor for miRNA24 sensing was 45 minutes. As shown in Figure 7A, the DPV signals decrease with the increasing of miRNA24 concentration, and the peak current changes [$\Delta I_p/I_0$] vary linearly with the logarithm of miRNA24 concentrations in the range from 1.0 fM to 1.0 pM. A

regression equation of y = 0.2623x + 1.722 (R^2 = 0.9876) was obtained with the sensitivity of 3.71 *ss* cm^{-2}, where y is the $\Delta I_p/I_0$ value and x is the logarithmic of miRNA24 concentration (nM), as demonstrated in Figure 7B. The limit of detection (LOD) is calculated to be as low as 0.34 fM (S/N=3). The CV method was also used to detect miRNA24 concentration. The linear regression equation of y=0.2096x+1.187 (R^2=0.9942) (R^2 = 0.9876) was obtained and the linear range is 0.1 pM - 0.1 nM with the LOD of 0.033 pM and the sensitivity of 2.96 *ss* cm^{-2}. Obviously, DPV method has wider linear range, lower LOD and higher sensitivity compared to CV method. The biosensing achievement of this biosensor was compared with previous biosensors reported (Table S1). The good biosensing performance of biosensor results from the following reasons: firstly, PA, with excellent biocompatibility and eco-friend, can provide friendly surroundings for DNA probes to maintain high binding a□nity and bioactivity [45]. Secondly, PANI/PA nanoplatform, as a stable substrate for biosensor, was firmly deposited onto GCE surface by a simple electrochemical strategy, which can provide numerous amino of synthetic hydrogel as the biding sites for DNA probe immobilization. A high fixed quantity of biomolecules, high and specific binding a□nity, and good bioactivity indicate that the constructed biosensor guarantee an ultra-low detection limit.

Fig. 7

To evaluate the selectivity of GCE/PANI/PA/DNA, the biosensor was exposed to solutions containing M1, M2, M3 and target miRNA24, separately, and monitored the changes in current. As shown in Figure S4, GCE/PANI/PA/DNA shows the

largest response towards miRNA24, and can successfully distinguish M1, M2 and M3.

The long-term stability and reproducibility are two important criteria to assess a successful biosensor for practical application. So as to investigate the reproducibility of GCE/PANI/PA/DNA, five biosensors developed independently were used to assay miRNA24 (0.10 nM), and the relative standard deviation (RSD) was 3.9%. The biosensors were used to detect the same target miRNA24 repetitively for seven times, and the RSD was 2.6%, proving good reproducibility. As shown in Figure S5, a longer-term analysis result of the biosensors across six days shows a retention of >91% signals.

4. Conclusion

In summary, PANI/PA hydrogel with mesoporous structure was prepared by one-step electrochemical method. In the conductive hydrogel, PANI inherent electroactivity, good conductivity and excellent chemical stability, while PA enables the hydrogel with good biocompatibility and antifouling property. Notably, the PANI/PA hydrogel can not only supply a large number active sites for DNA fixation, but also generate the inherent reduction and oxide signal from PANI as the electrochemical signal (without addition of other redox probes). A low-fouling and ultrasensitive electrochemical biosensor based on PANI/PA hydrogel has been developed for miRNA detection. This study provides an effective and reliable method for the construction of ultrasensitive

and antifouling biosensors, especially for the assay of biomarkers in real biological samples in practical applications.

Acknowledgments

This research was supported by the National Natural Science Foundation of China (21705088), major agricultural application technology innovation projects in Shandong Province (SD2019NJ001-2), the Shandong Science and Technology Program (J14LB14), the Qingdao Agricultural University High-level Talent Project (663/1117025).

References

[1] S.X. Wang, D. Acha, A.J. Shah, F. Hills, I. Roitt, A. Demosthenous, et al., Detection of the tau protein in human serum by a sensitive four-electrode electrochemical biosensor, Biosens. Bioelectron. 92 (2016) 482-488.

[2] M. Li, M. Lv, L. Wang, C. Fan, X. Zuo, Engineering electrochemical interface for biomolecular sensing, Curr. Opin. Electrochem. 14 (2019) 71-80.

[3] H.C. Wu, W. Xiaoyuan, G. Bingyuan, S. Yingying, W. Jin, P. Shuchuan, et al., Multiplexed discrimination of microRNA single nucleotide variants through triplex molecular beacon sensors, Chem. Commun. 54 (2018) 7673-7676

[4] A.L. Morgado, C.M. Rodrigues, S. Solá, MicroRNA-145 Regulates Neural Stem Cell Differentiation Through the Sox2-Lin28/let-7 Signaling Pathway, Stem Cells 34 (2016) 1386-1395..

[5] D.W. Trobaugh, W.B. Klimstra, MicroRNA Regulation of RNA Virus Replication and Pathogenesis, Trends Mol. Med. 23 (2017) 80-93.

[6] S. Sylvia, C.W. Michalski, E. Mert, K. Jörg, F. Helmut, Northern blot analysis for detection and quantification of RNA in pancreatic cancer cells and tissues, Nat. Protoc. 4 (2009) 37-43.

[7] E. Mishima, D. Jinno, Y. Akiyama, K. Itoh, S. Nankumo, H. Shima, et al., Immuno-Northern Blotting: Detection of RNA Modifications by Using Antibodies against Modified Nucleosides, Plos One 10 (2015) e0143756.

[8] N.S. Maan, S. Maan, M. Belaganahalli, G. Pullinger, A.J.A. Montes, M.R. Gasparini, et al., A quantitative real-time reverse transcription PCR (qRT-PCR) assay to detect genome segment 9 of all 26 bluetongue virus serotypes, J. Virol. Methods 213 (2015) 118-126.

[9] M. Peng, Y. Tang, Z. Mao, Y. Liu, Adamantane Derivatives Functionalized Gold Nanoparticles for Colorimetric Detection of MiRNA, Part Part Syst. Charact. 34 (2017) 1600405.

[10] W. Yanqin, X. Yan, M. Xiuhai, W. Yingliang, S. Haiyun, C. Nan, et al., DNAzyme-based rolling-circle amplification DNA machine for ultrasensitive analysis of microRNA in Drosophila larva, Anal. Chem. 84 (2012) 7664-7669.

[11] G. Donadio, R. Di Martino, R. Oliva, L. Petraccone, P. Del Vecchio, B. DI LUCCIA, et al., A new peptide-based fluorescent probe selective for zinc (II) and copper (II), J. Mater. Chem. B 4 (2016) 6979-6988

[12] W. Yang, W. Guo, J. Chang, B. Zhang, Protein / Peptide-Templated Biomimetic Synthesis of Inorganic Nanoparticles for Biomedical Applications, J. Mater. Chem. B 5 (2017) 401-17

[13] C.S. Fang, K.S. Kim, B. Yu, S. Jon, M.S. Kim, H. Yang, Ultrasensitive Electrochemical Detection of miRNA-21 Using a Zinc Finger Protein Specific to DNA-RNA Hybrids, Anal. Chem. 89 (2017) 2024-2031.

[14] M.N. Islam, V. Gopalan, M.H. Haque, M.K. Masud, M.S.A. Hossain, Y. Yamauchi, et al., A PCR-free electrochemical method for messenger RNA detection in cancer tissue samples, Biosens. Bioelectron. 98 (2017) 227-233.

[15] P. Gillespie, S. Ladame, D. O'Hare, Molecular methods in electrochemical microRNA detection, Analyst 144 (2019) 114-129.

[16] A. Abi, M. Lin, H. Pei, C. Fan, E.E. Ferapontova, X. Zuo, Electrochemical switching with 3D DNA tetrahedral nanostructures self-assembled at gold electrodes, ACS Appl. Mater. Interfaces 6 (2014) 8928-8931.

[17] S. Jiang, Z. Cao, Ultralow-fouling, functionalizable, and hydrolyzable zwitterionic materials and their derivatives for biological applications, Adv. Mater. 22 (2010) 920-932.

[18] S. Taufik, A. Barfidokht, M.T. Alam, J. Cheng, S.G. Parker, J.J. Gooding, An antifouling electrode based on electrode–organic layer–nanoparticle constructs: Electrodeposited organic layers versus self-assembled monolayers, J. Electroanal. Chem. 779 (2016) 229-235.

[19] C. Liu, J. Lee, J. Ma, M. Elimelech, Antifouling Thin-Film Composite Membranes by Controlled Architecture of Zwitterionic Polymer Brush Layer, Environ. Sci. Technol. 51 (2017) 2161-2169.

[20] Y. Higaki, M. Kobayashi, D. Murakami, A. Takahara, Anti-fouling behavior of polymer brush immobilized surfaces, Polym J. 48 (2016) 325-231.

[21] C. Min, W. Yu, H. Wang, Y. Wu, X. Luo, A label-free electrochemical DNA

biosensor for breast cancer marker BRCA1 based on self-assembled antifouling peptide monolayer, Sens. Actuators, B 244 (2017) 742-749.

[22] N. Hui, X. Sun, S. Niu, X. Luo, PEGylated Polyaniline Nanofibers: Antifouling and Conducting Biomaterial for Electrochemical DNA Sensing, ACS Appl. Mater. Interfaces 9 (2017) 2914-2923.

[23] L. Li, Y. Shi, L. Pan, Y. Shi, G. Yu, Rational design and applications of conducting polymer hydrogels as electrochemical biosensors, J. Mater. Chem. B 3 (2015) 2920-2930.

[24] M.C. Cushing, K.S. Anseth, Hydrogel cell cultures, Science 316 (2007) 1133-1134.

[25] M.C. Koetting, J.T. Peters, S.D. Steichen, N.A. Peppas, (2015). Stimulus-responsive hydrogels: theory, modern advances, and applications, Mater. Sci.Eng. 93 (2015) 1-49.

[26] Y. Shi, M. Wang, C.B. Ma, Y.Q. Wang, X.P. Li, G.H. Yu, A conductive self-healing hybrid gel enabled by metal-ligand supramolecule and nanostructured conductive polymer, Nano Lett. 15 (2015) 6276-6281.

[27] P. Marcasuzaa, S. Reynaud, F. Ehrenfeld, A. Khoukh, J. Desbrieres, Chitosan-graft-polyaniline-based hydrogels: elaboration and properties, Biomacromolecules 11 (2010) 1684-1691.

[28] L. Liu, S. Luo, Y. Qing, N. Yan, Y. Wu, X. Xie, et al., A Temperature-Controlled, Conductive PANI@CNFs/MEO 2 MA/PEGMA Hydrogel for Flexible Temperature Sensors, Macromol Rapid Commun. 39 (2018) e1700836.

[29] Y. Wang, X. Yang, Q. Ling, L. Dan, Revisiting the capacitance of polyaniline by using graphene hydrogel films as a substrate: The importance of nano-architecturing, Energy Environ. Sci. 6 (2013) 477-481.

[30] W. Li, F. Gao, X. Wang, N. Zhang, M. Ma, Strong and Robust Polyaniline□Based Supramolecular Hydrogels for Flexible Supercapacitors, Angew. Chem. 128 (2016) 9342-9347.

[31] A.J. Hatch, J.D. York, SnapShot: Inositol phosphates, Cell 143 (2010) 1030.e1.

[32] L. Pan, G. Yu, D. Zhai, H.R. Lee, W. Zhao, N. Liu, et al., Hierarchical

nanostructured conducting polymer hydrogel with high electrochemical activity, Proc. Natl. Acad. Sci. U S A 109 (2012) 9287-9292.

[33] X. Wang, K. Wen, X. Yang, L. Li, X. Yu, Biocompatibility and anti-calcification research of a biological artery fixed with natural-occurred phytic acid as crosslinking reagent, J. Mater. Chem. B 5 (2017) 8115-8124.

[34] X. Song, Y. Chen, M. Rong, Z. Xie, T. Zhao, Y. Wang, et al., A Phytic Acid Induced Super-Amphiphilic Multifunctional 3D Graphene-Based Foam, Angew. Chem. Int. Ed. Engl. 55 (2016) 3936-3941.

[35] L. Li, G. Zhang, Z. Su, One-Step Assembly of Phytic Acid Metal Complexes for Superhydrophilic Coatings, Angew. Chem. Int. Ed. 55 (2016) 9093-9096.

[36] E. Pringsheim, E. Terpetschnig, S. A. Piletsky, O. S. Wolfbeis, A Polyaniline with Near-Infrared Optical Response to Saccharides, Adv. Mater. 1999, 11, 865-868.

[37] N. Liu, J. Song, Y. Lu, J.J. Davis, F. Gao, X. Luo, Electrochemical Aptasensor for Ultralow Fouling Cancer Cell Quantification in Complex Biological Media Based on Designed Branched Peptides, Anal. Chem. 91 (2019) 8334-8340.

[38] X. Xuan, H.S. Yoon, J.Y. Park, A Wearable Electrochemical Glucose Sensor based on Simple and Low-Cost Fabrication Supported Micro-Patterned Reduced Graphene Oxide Nanocomposite Electrode on Flexible Substrate, Biosens. Bioelectron. 109 (2018) 75-82.

[39] M.A. Deshmukh, M. Gicevicius, A. Ramanaviciene, M.D. Shirsat, R. Viter, A. Ramanavicius, Hybrid electrochemical/electrochromic Cu(II) ion sensor prototype based on PANI/ITO-electrode, Sens. Actuators, B 248 (2017) 527-535.

[40] K. Yu, T. Okanishi, H. Muroyama, T. Matsui, K. Eguchi, Enhanced Supply of Hydroxyl Species in CeO 2 -Modified Platinum Catalyst Studied by in situ ATR-FTIR Spectroscopy, ACS Catal. 6 (2016) 2026-2034.

[41] S. Chen, L. Li, C. Zhao, J. Zheng, Surface hydration: Principles and applications toward low-fouling/nonfouling biomaterials, Polymer 51 (2010) 5283-5293.

[42] J. Deng, T. Wang, J. Guo, L. Peng, Electrochemical capacity fading of polyaniline electrode in supercapacitor: An XPS analysis, Prog. Nat. Sci: Mater. Int. 27 (2017) 257-260.

[43] M.J.A. Shiddiky, P.H. Kithva, D. Kozak, M. Trau, An electrochemical immunosensor to minimize the nonspecific adsorption and to improve sensitivity of protein assays in human serum, Biosens. Bioelectron. 38 (2012) 132-137.

[44] H.Q.A. Lê, S. Chebil, B. Makrouf, H. Sauriat-Dorizon, B. Mandrand, H. Korri-Youssoufi, Effect of the size of electrode on electrochemical properties of ferrocene-functionalized polypyrrole towards DNA sensing, Talanta 81 (2010) 1250-1257.

[45] H. Dai, W. Nan, D. Wang, H. Ma, L. Meng, An electrochemical sensor based on phytic acid functionalized polypyrrole/graphene oxide nanocomposites for simultaneous determination of Cd(II) and Pb(II), Chem. Eng. J. 299 (2016) 150-155.

Captions

Scheme 1 The description of structure of PANI/PA antifouling interface and its application for miRNA24 sensor.

Fig. 1 (A) Synthesis of boronate-bearing PANI by copolymerization of ABA and aniline. (B) SEM images (a, b) (low and high magnification images) and chemical structure (c) of electrodes modified with PANI/PA hydrogels.

Fig. 2 (A) FTIR spectrum of PANI (curve a) and PANI/PA nanocomposite (curve b). (B) The cyclic voltammetry curve of PANI/PA swept in PBS 5.7. (C) Static water contact angles of bare electrode (a), PANI (b), and PANI/PA (c) surfaces.

Fig. 3 XPS spectra of PANI (A), PANI/PA (B), and PANI/PA/DNA (C).

Fig. 4 The changes of DPV response of PANI (A) and PANI/PA (B) before (black line) and after (red line) soaking in single protein solution (1: BHb; 2: BSA; 3: HSA; 4: Lys; 10^{-6} g mL^{-1}).

Fig. 5 The fluorescence microscopy versions of GCE, GCE/PANI, and GCE/PANI/PA after soaking in FITC-BSA solution (0.1 mg mL^{-1}) for 30 minutes.

Fig. 6 CV (A) and DPV (B) curves recorded in PBS 5.7. (a, PANI/PA; b, PANI/PA/DNA; c, PANI/PA/DNA/miRNA). (C) CVs of the electrode modified by PANI/PA in PBS (0.2 M, pH 5.7) at di□erent scan rates from 0.1 to 2.5 V s^{-1}. (D) The relations of the PANI/PA modified GCEs with the anodic and cathodic peak current against the scan rate.

Fig. 7 (A) DPV responses of GCE/PANI/PA/DNA to miRNA24. Curve a represent the blank solution and curves b-i refer to miRNA24 concentrations from 1 fM to 10 nM. (B) The corresponding calibration curve of the biosensor with different concentration of miRNA24 in PBS 5.7. (C) CV responses of the PANI/PA/DNA to miRNA24. Curve a represent the blank solution and curves b-h refer to miRNA24 concentrations from 100 fM to 1 nM. (D) The corresponding calibration curve of the biosensor with different concentration of RNA24 in PBS 5.7.

Scheme 1

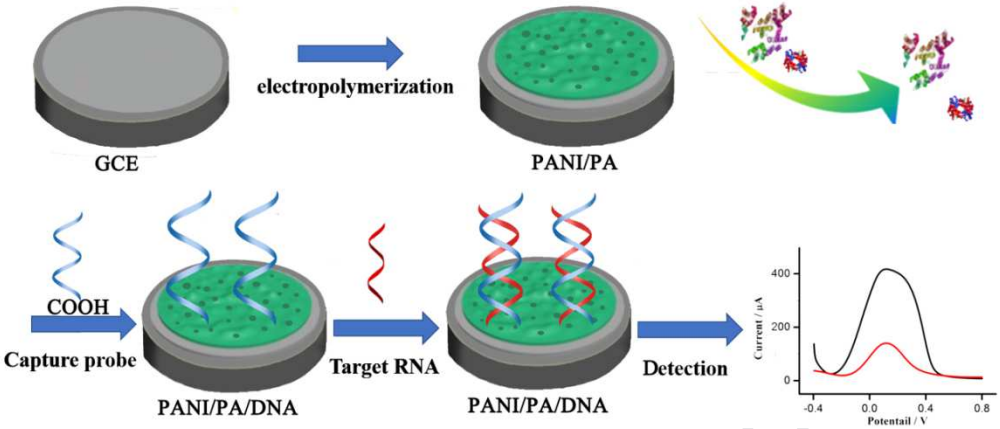

Fig. 1

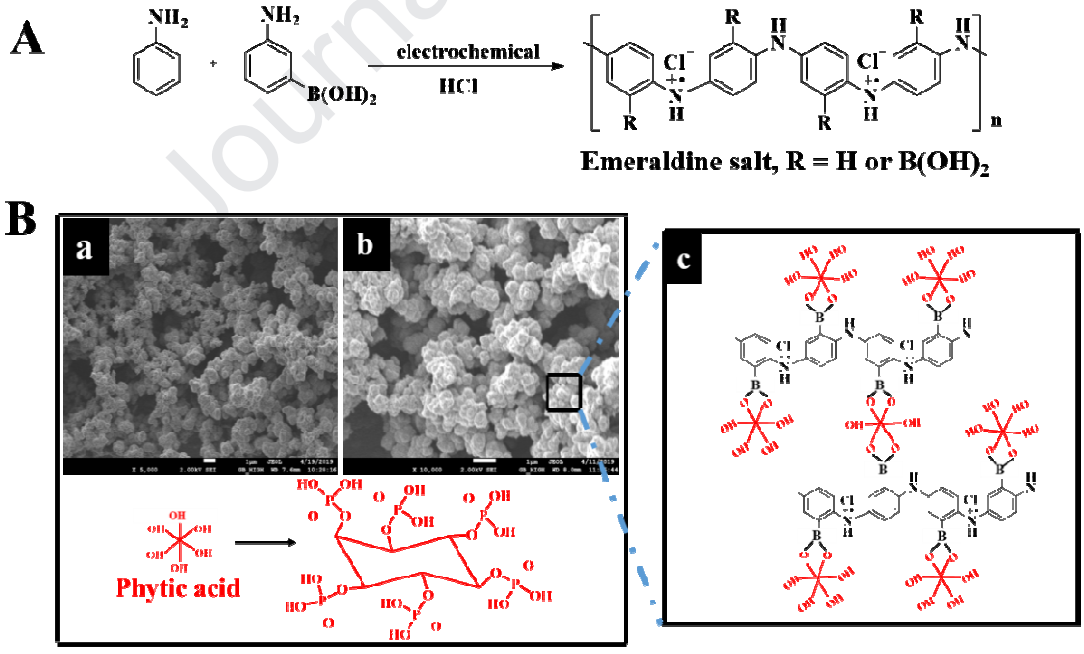

Fig. 2

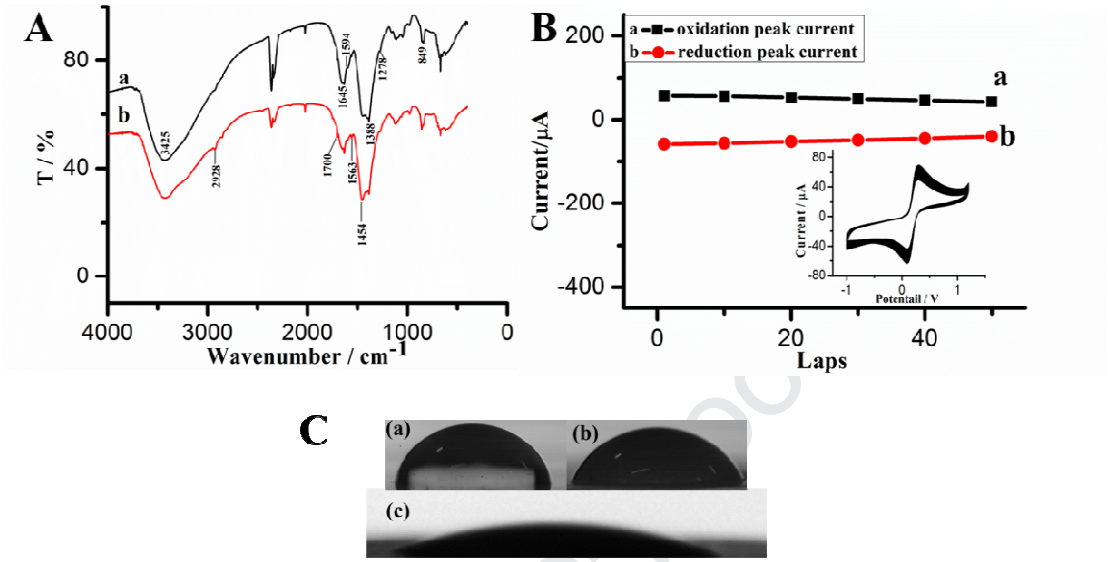

Fig. 3

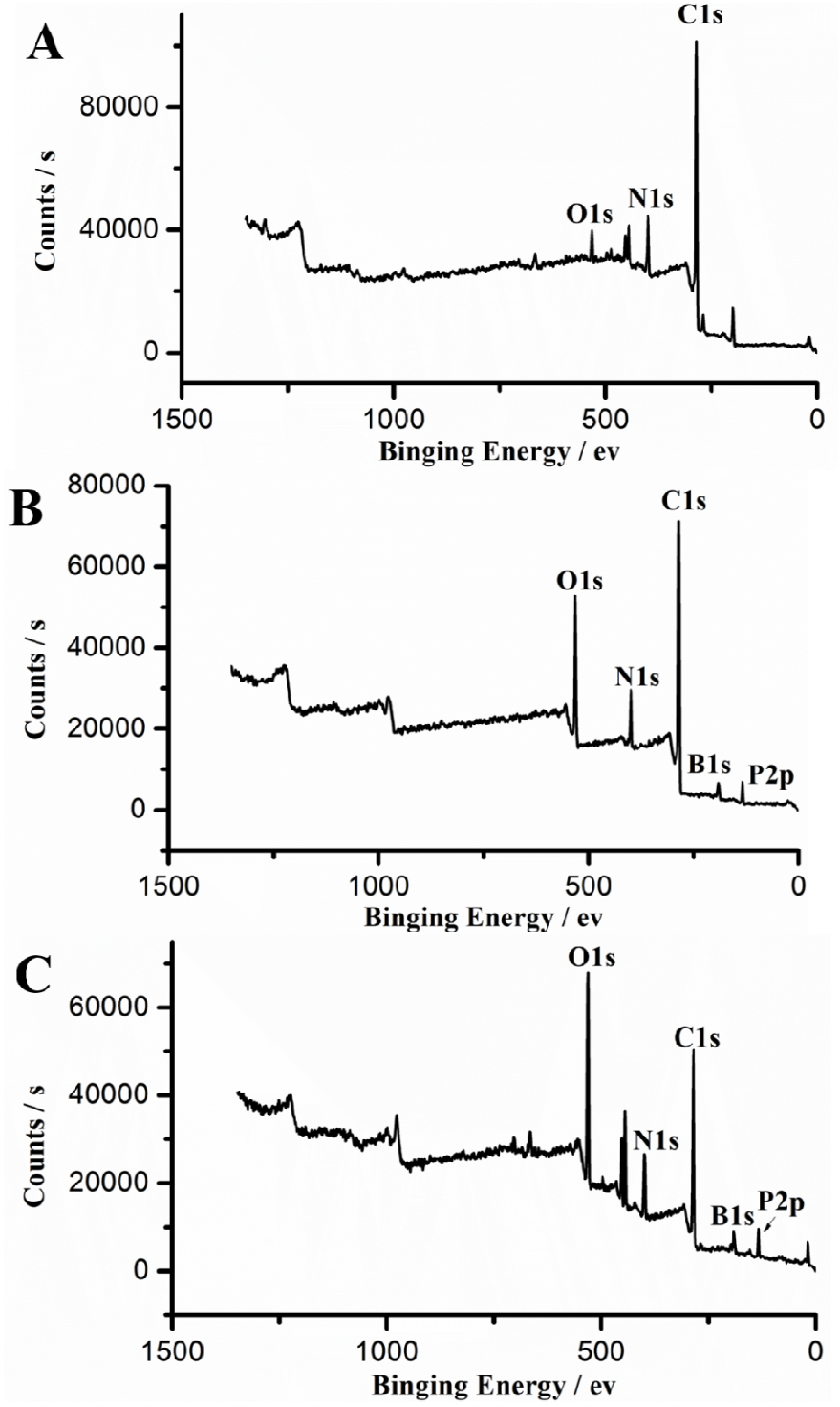
A
C1s
O1s
N1s
Counts / s
80000
40000
0
1500
1000
500
0
Binging Energy / ev
B
C1s
O1s
N1s
B1s
P2p
Counts / s
80000
60000
40000
20000
0
1500
1000
500
0
Binging Energy / ev
C
O1s
C1s
N1s
B1s
P2p
Counts / s
60000
40000
20000
0
1500
1000
500
0
Binging Energy / ev

Fig. 4

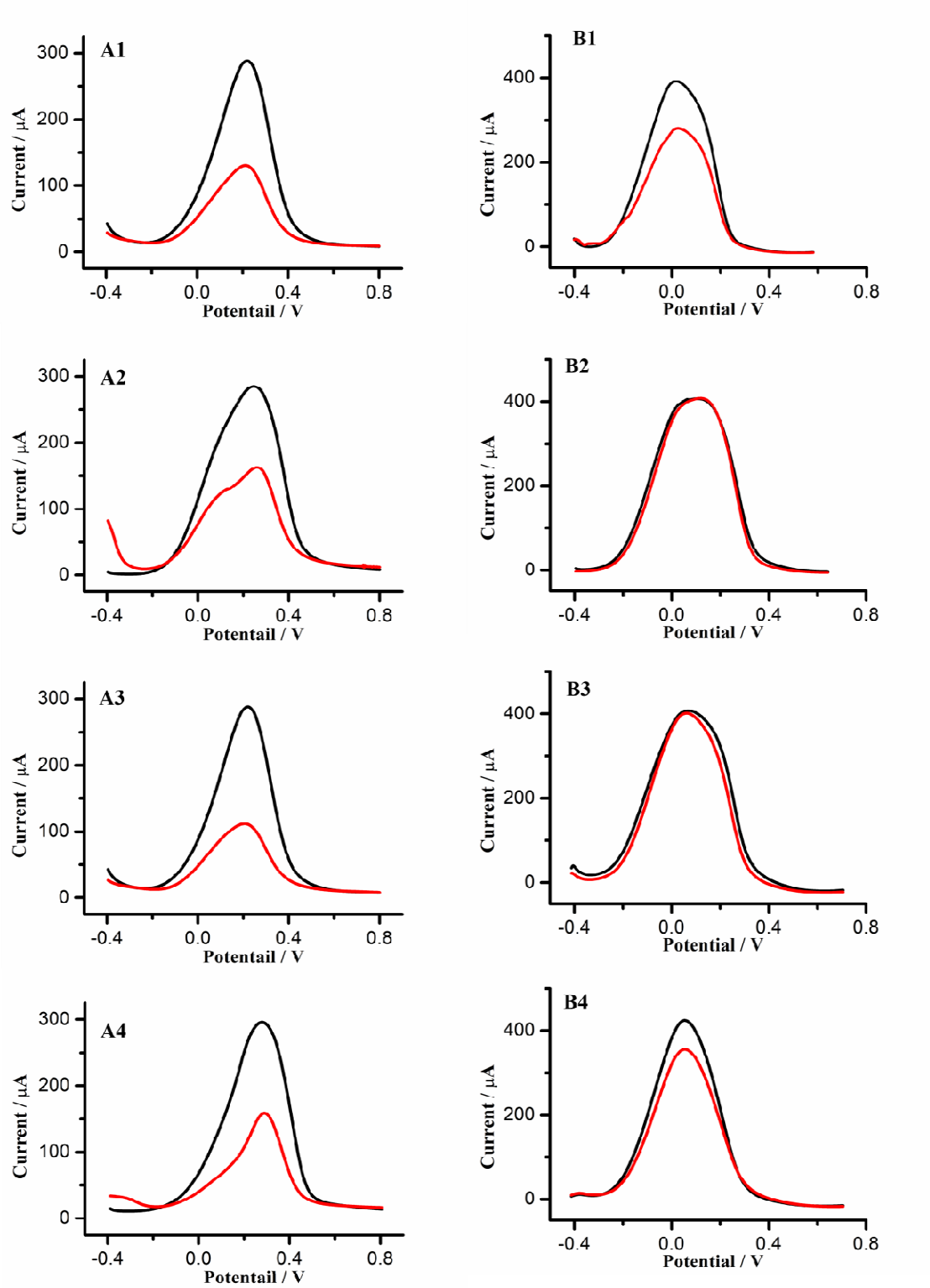
A1
B1
A2
B2
A3
B3
A4
B4
Current / μA
Potentail / V
Potential / V
300
200
100
0
400
-0.4
0.0
0.4
0.8

Fig. 5

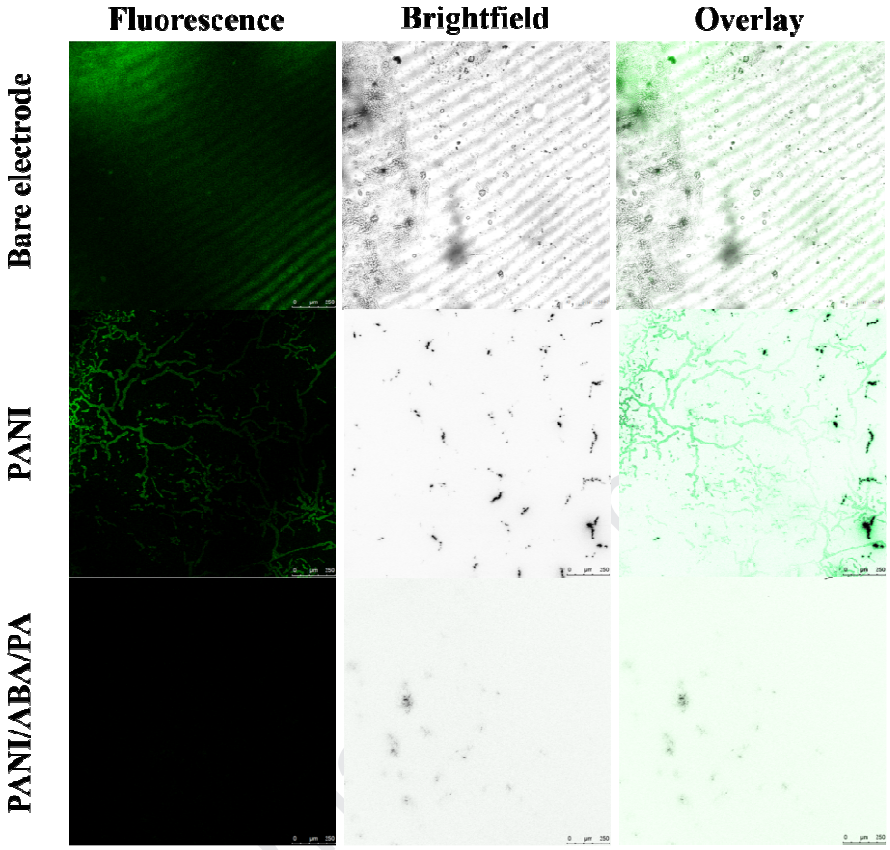
Fluorescence
Brightfield
Overlay
Bare electrode
PANI
PANI/ABA/PA

Fig. 6

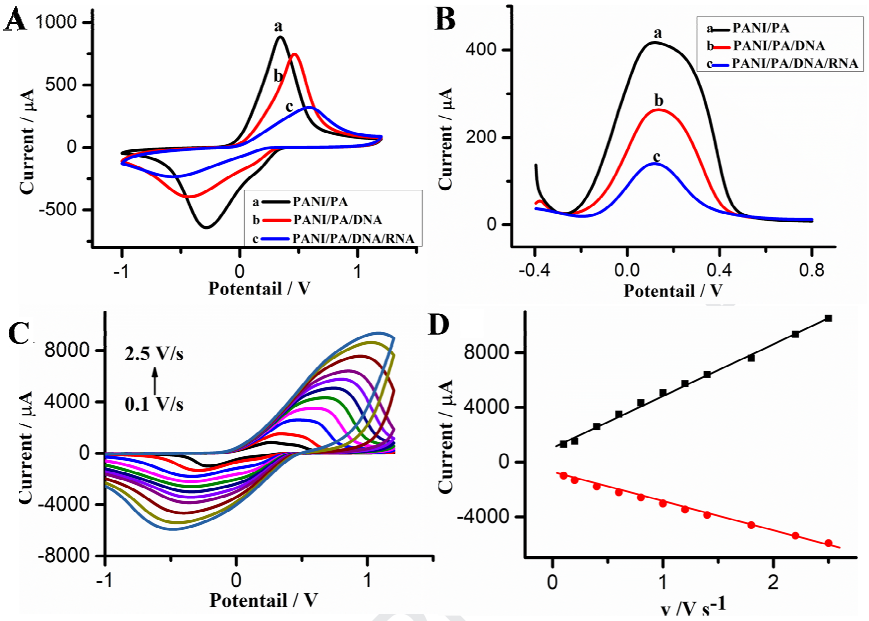
A
B
C
D
Current / μA
Potentail / V
a PANI/PA
b PANI/PA/DNA
c PANI/PA/DNA/RNA
2.5 V/s
0.1 V/s
v /V s-1

Fig. 7

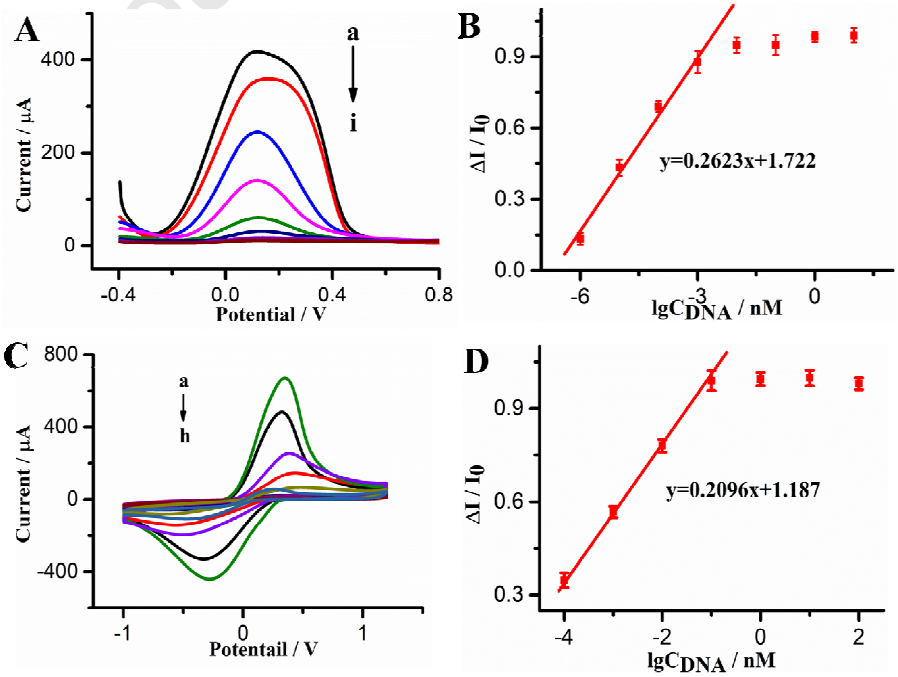
A
B
C
D
Current / μA
Potential / V
Potentail / V
ΔI / I0
y=0.2623x+1.722
y=0.2096x+1.187
lgCDNA / nM

A

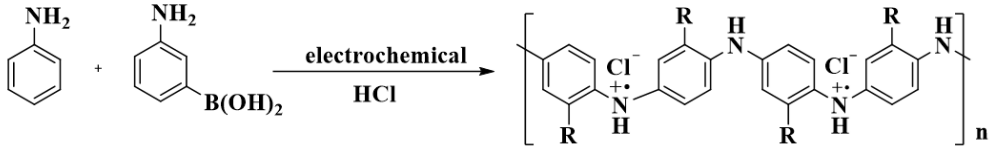

Emeraldine salt, R = H or $B(OH)_2$

B

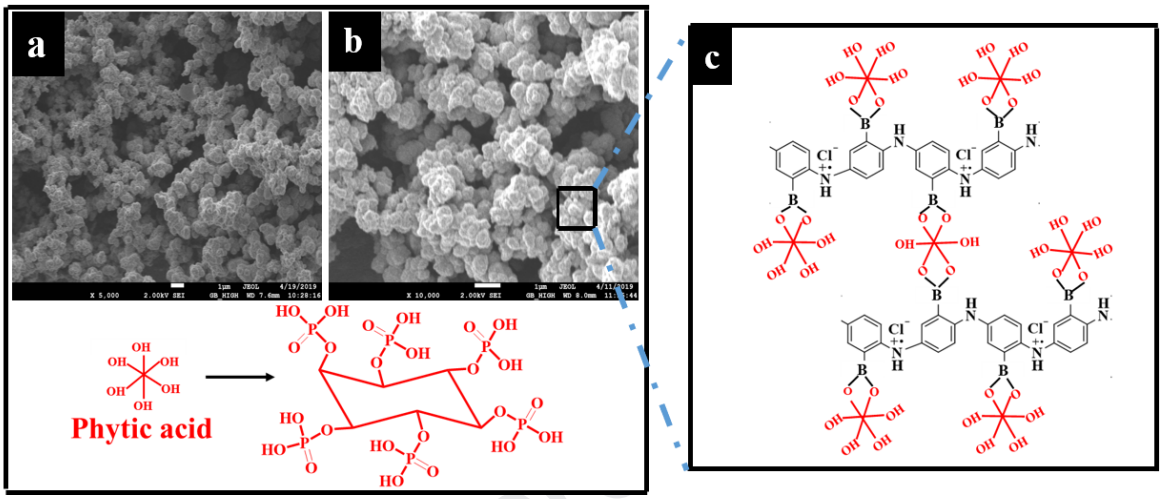

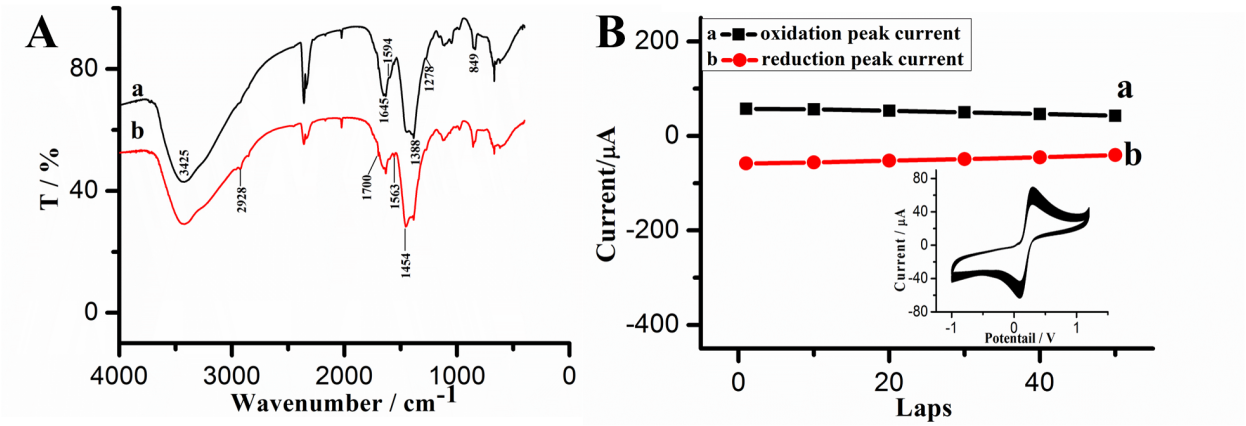

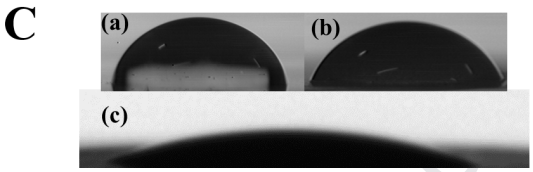

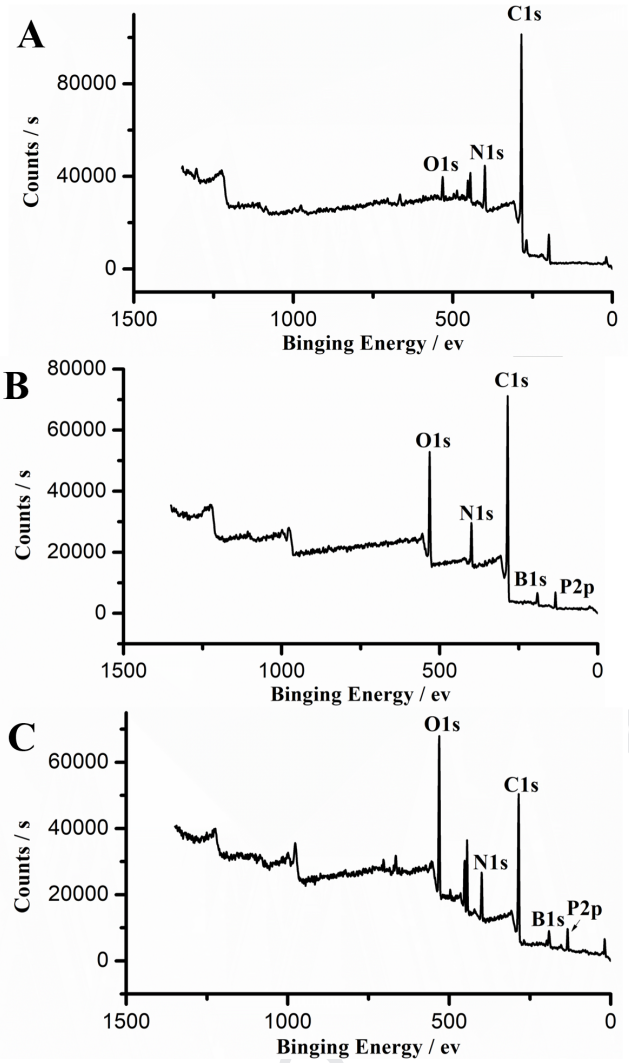

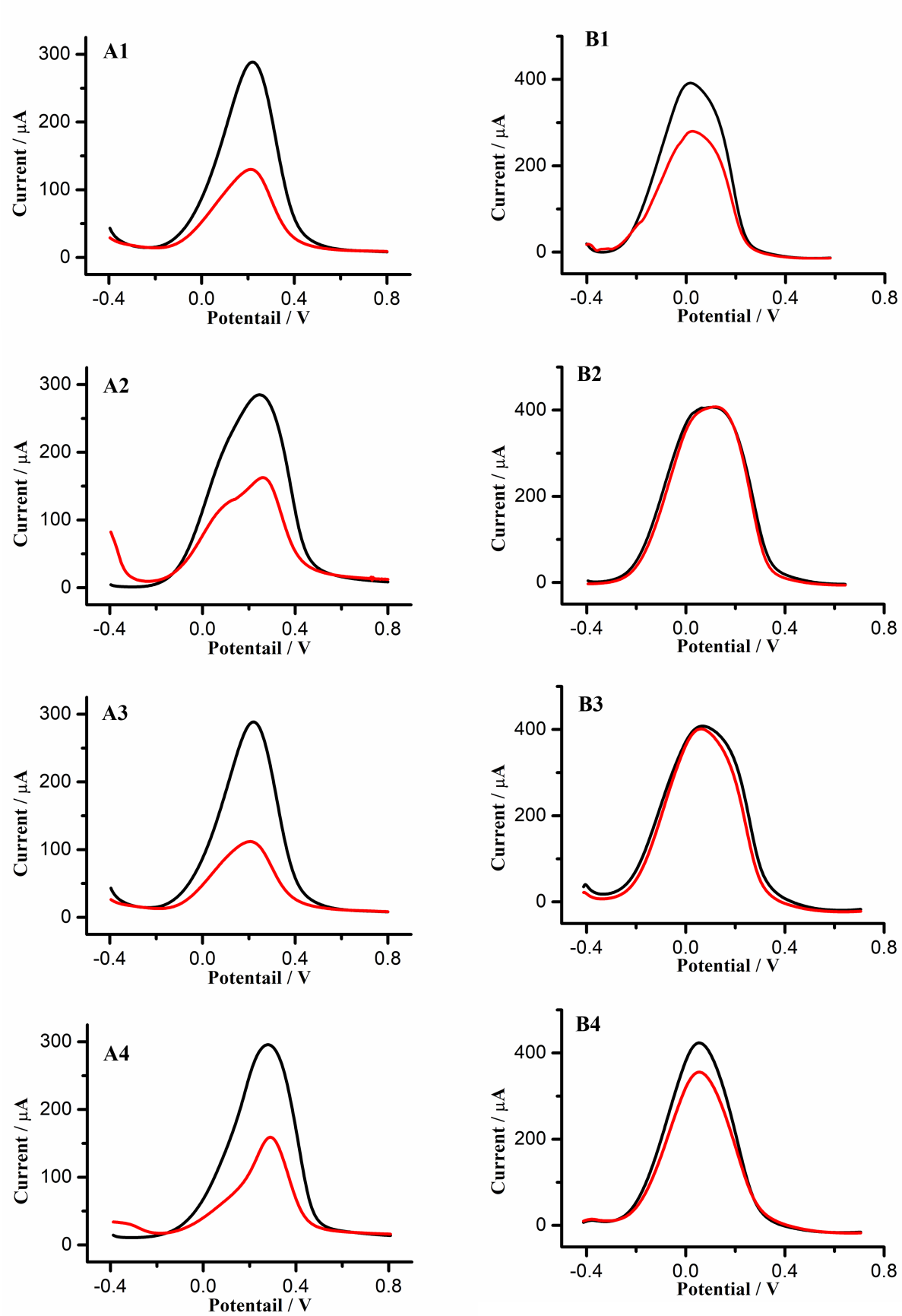
A1
B1
A2
B2
A3
B3
A4
B4
Current / μA
Potentail / V
Potential / V
300
200
100
0
400
-0.4
0.0
0.4
0.8

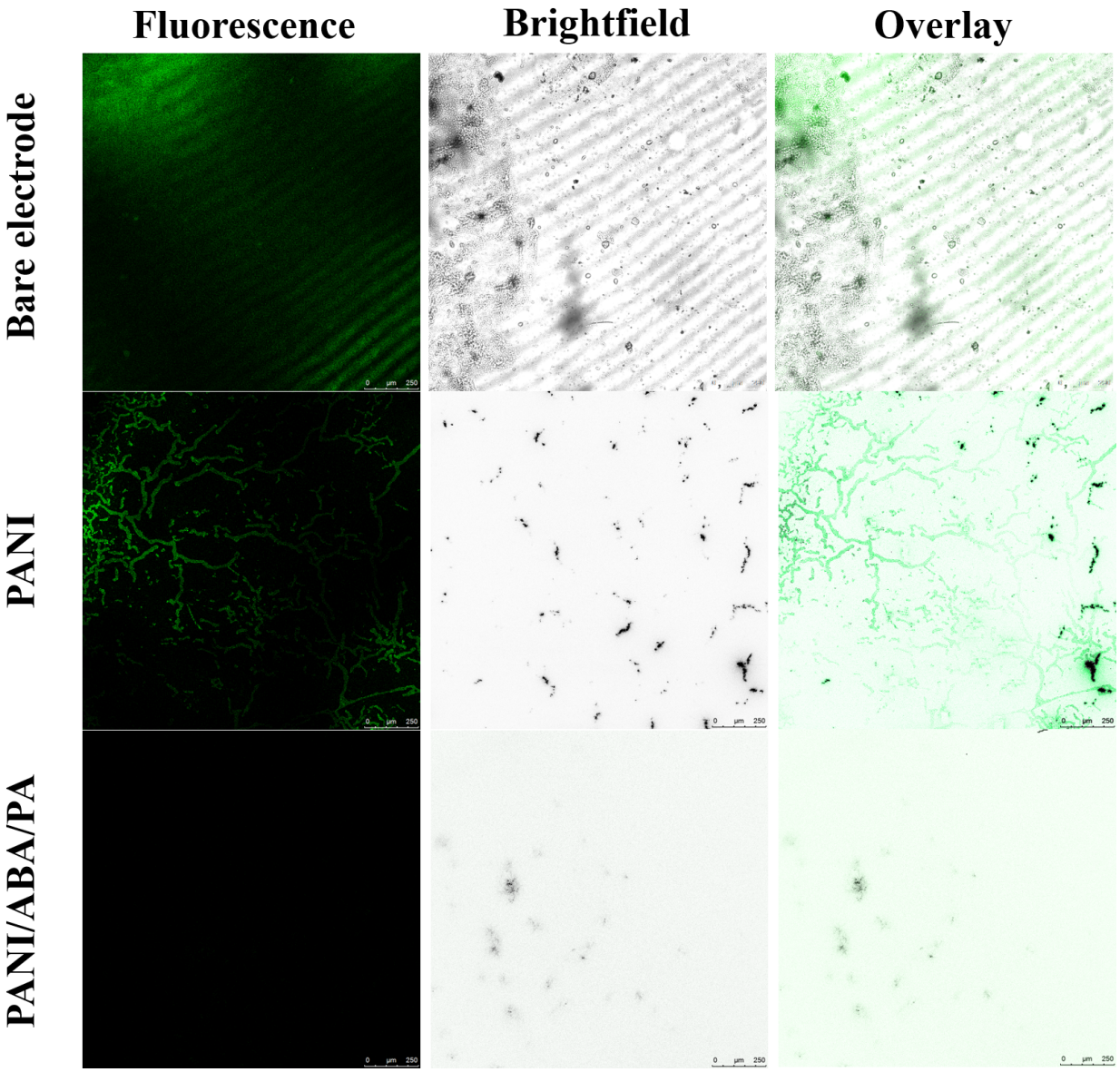
Fluorescence
Brightfield
Overlay
Bare electrode
PANI
PANI/ABA/PA
0 µm 250

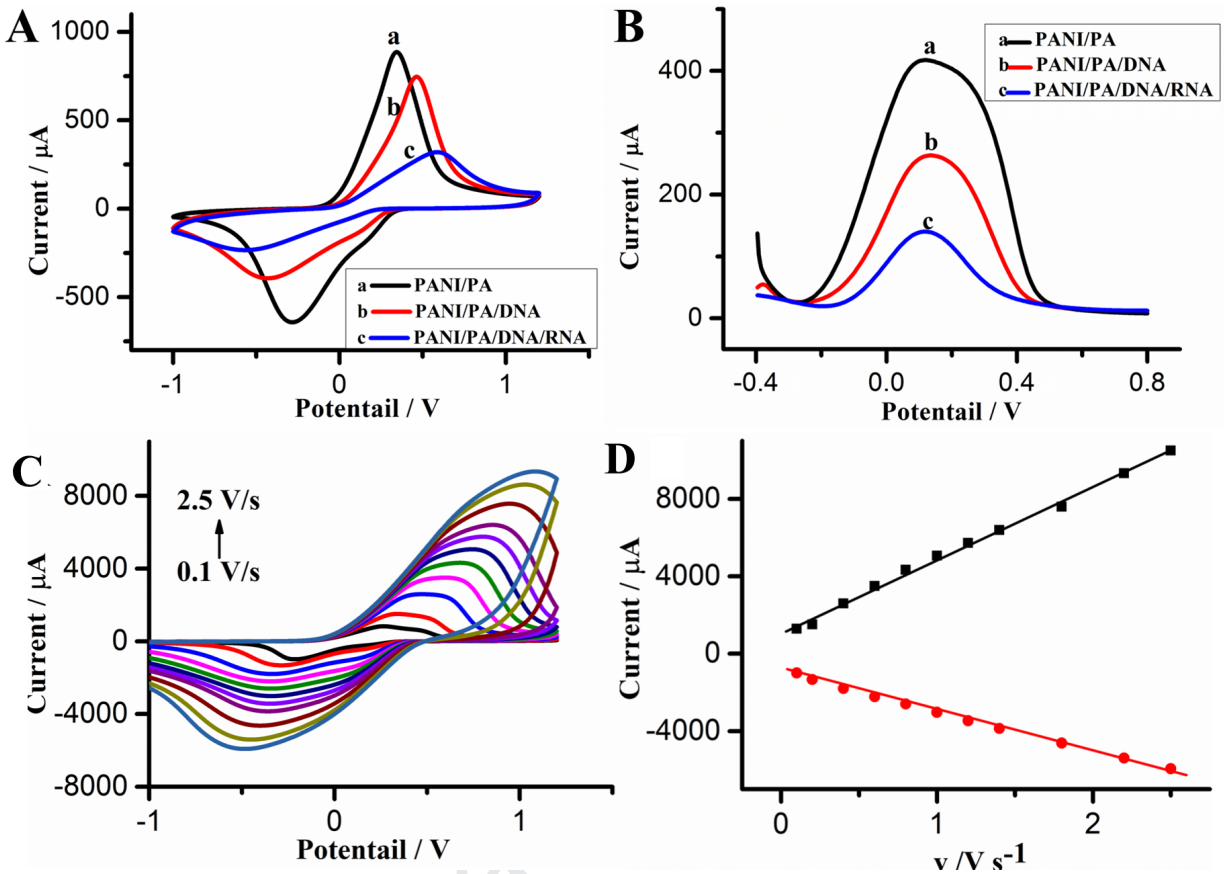
A
Current / μA
Potentail / V
a PANI/PA
b PANI/PA/DNA
c PANI/PA/DNA/RNA
B
Current / μA
Potentail / V
a PANI/PA
b PANI/PA/DNA
c PANI/PA/DNA/RNA
C
Current / μA
Potentail / V
2.5 V/s
0.1 V/s
D
Current / μA
v /V s-1

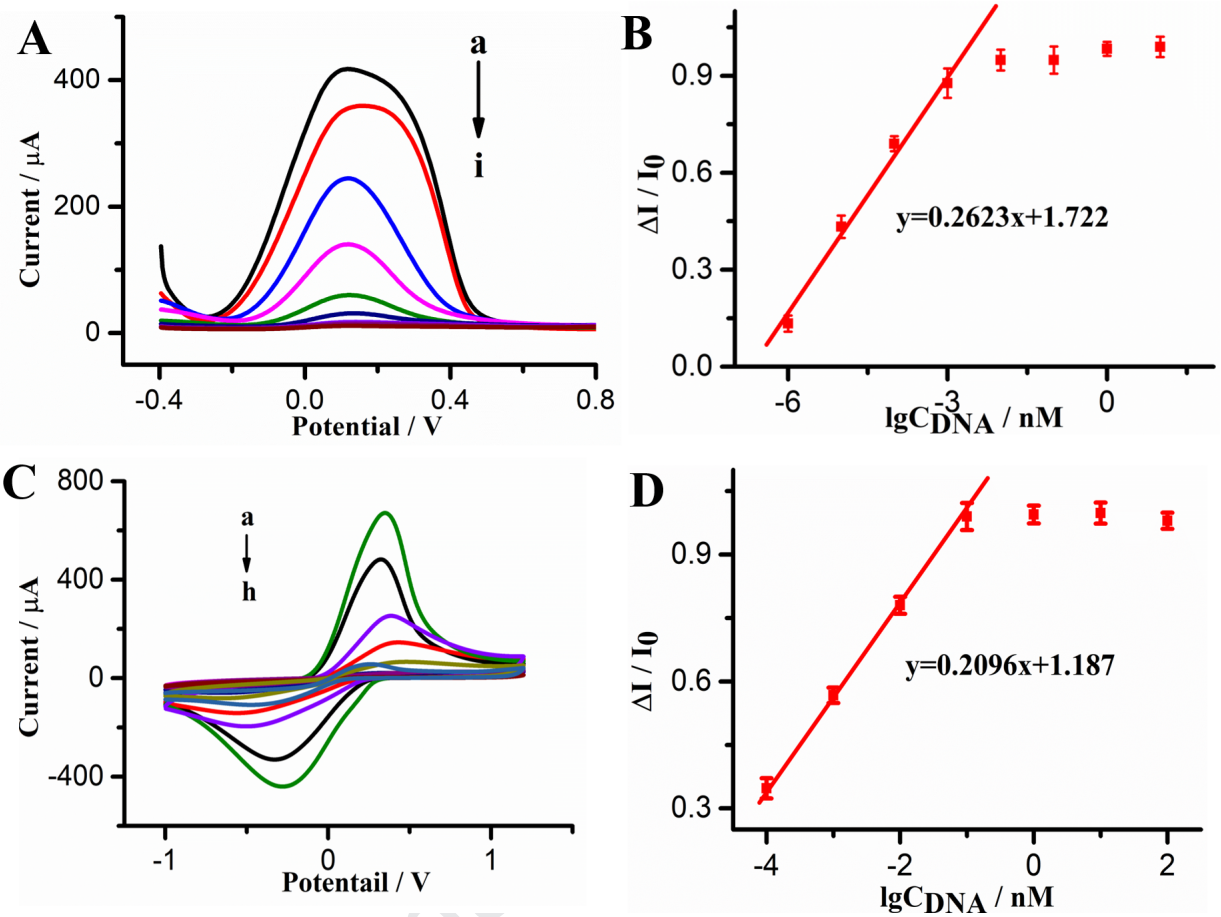
A
a
i
Current / μA
400
200
0
-0.4
0.0
0.4
0.8
Potential / V
B
ΔI / I0
0.9
0.6
0.3
0.0
y=0.2623x+1.722
-6
-3
0
lgCDNA / nM
C
a
h
Current / μA
800
400
0
-400
-1
0
1
Potentail / V
D
ΔI / I0
0.9
0.6
0.3
y=0.2096x+1.187
-4
-2
0
2
lgCDNA / nM

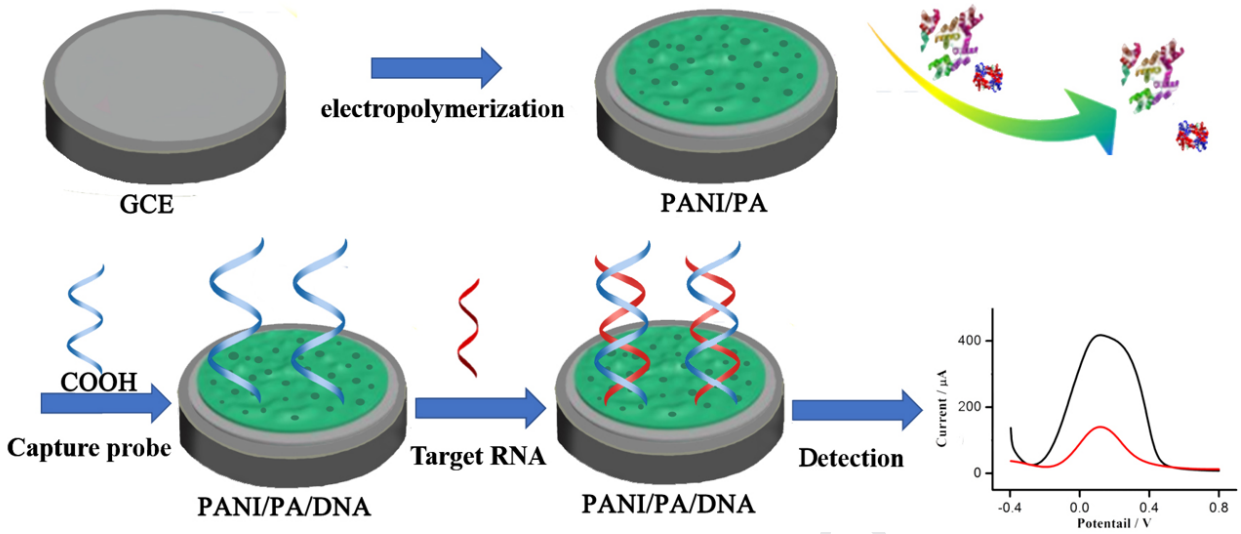

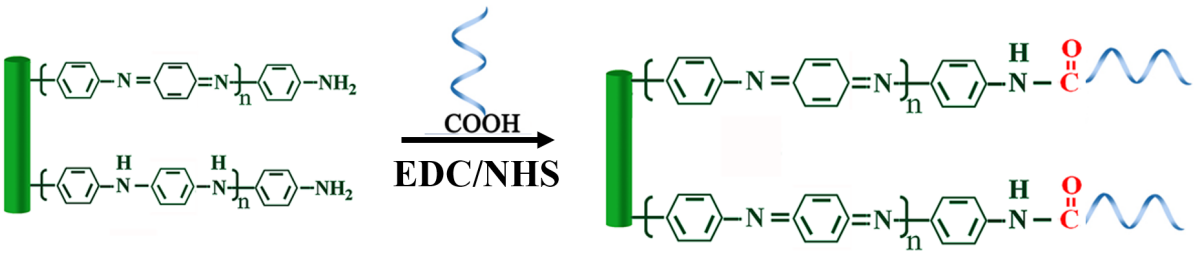

Highlights

1. Conducting polymer hydrogel PANI/PA was prepared by one-step electrochemical copolymerization way.

2. The PANI/PA hydrogel demonstrated antifouling property towards four single protein and two complex biological media.

3. The low fouling, label-free biosensor based on PANI/PA hydrogel has been constructed for MicroRNA24.

4. The biosensor based on PANI/PA hydrogel has shown excellent sensing performances with wide linear range (1.0 fM-1.0 pM) and low sensing limit (0.34 fM).

Declaration of interests

☒ The authors declare that they have no known competing financial interests or personal relationships that could have appeared to influence the work reported in this paper.

☐The authors declare the following financial interests/personal relationships which may be considered as potential competing interests: